OPEN

Molecular Psychiatry (2016) 21, 97–107

www.nature.com/mp

ORIGINAL ARTICLE

A_{2A} adenosine receptor deletion is protective in a mouse model of Tauopathy

C Laurent[1,2,11], S Burnouf[1,2,11], B Ferry[3,12], VL Batalha[4,12], JE Coelho[4,12], Y Baqi[5,6], E Malik[5], E Mariciniak[1,2], S Parrot[3,7], A Van der Jeugd[8], E Faivre[1,2], V Flaten[1,2], C Ledent[9], R D'Hooge[8], N Sergeant[1,2,10], M Hamdane[1,2,10], S Humez[1,2], CE Müller[5], LV Lopes[4], L Buée[1,2,10] and D Blum[1,2,10]

Consumption of caffeine, a non-selective adenosine A_{2A} receptor (A_{2A}R) antagonist, reduces the risk of developing Alzheimer's disease (AD) in humans and mitigates both amyloid and Tau burden in transgenic mouse models. However, the impact of selective A_{2A}R blockade on the progressive development of AD-related lesions and associated memory impairments has not been investigated. In the present study, we removed the gene encoding A_{2A}R from THY-Tau22 mice and analysed the subsequent effects on both pathological (Tau phosphorylation and aggregation, neuro-inflammation) and functional impairments (spatial learning and memory, hippocampal plasticity, neurotransmitter profile). We found that deleting A_{2A}Rs protect from Tau pathology-induced deficits in terms of spatial memory and hippocampal long-term depression. These effects were concomitant with a normalization of the hippocampal glutamate/gamma-amino butyric acid ratio, together with a global reduction in neuro-inflammatory markers and a decrease in Tau hyperphosphorylation. Additionally, oral therapy using a specific A_{2A}R antagonist (MSX-3) significantly improved memory and reduced Tau hyperphosphorylation in THY-Tau22 mice. By showing that A_{2A}R genetic or pharmacological blockade improves the pathological phenotype in a Tau transgenic mouse model, the present data highlight A_{2A} receptors as important molecular targets to consider against AD and Tauopathies.

Molecular Psychiatry (2016) **21,** 97–107; doi:10.1038/mp.2014.151; published online 2 December 2014

INTRODUCTION

Consumption of the methylxanthine caffeine is beneficial in age-related cognitive decline.[1] More importantly, longitudinal and retrospective epidemiological studies show that it delays dementia onset and reduces Alzheimer's disease (AD) risk.[1] Consistent with these epidemiological observations, chronic treatment with caffeine in AD animal models improves memory and mitigates accumulation of amyloid peptides and hyperphosphorylated Tau proteins, the two neuropathological hallmarks of this disorder.[2,3]

Caffeine is a non-selective adenosine A_{2A} receptor (A_{2A}R) antagonist.[4] A_{2A}Rs are constitutively activated G-protein-coupled receptors, preferentially expressed in striato-pallidal medium spiny neurons, but are also present, to a lower extent, in cortical and hippocampal neurons.[5] Neuronal A_{2A}Rs modulate excitability by pre-synaptic control of neurotransmitter release, notably glutamate, as well as by post-synaptic control of excitability.[6,7] A_{2A}Rs are also expressed by astrocytes and microglia, controlling their activation state and their ability to uptake glutamate or to release pro-inflammatory factors.[6] Blockade of A_{2A}Rs has been shown to afford neuroprotection in various neurodegenerative conditions, such as stroke and Parkinson's disease.[8] Interestingly, the protective effects of caffeine achieved in Parkinson's disease models are mimicked by A_{2A}R pharmacological blockade and gene deletion.[9,10] In sharp contrast, the amount of data regarding the impact of A_{2A}R modulation in AD is still scarce. So far, A_{2A}R blockade was found to be protective against the acute toxicity of amyloid peptides.[11] However, the impact of A_{2A}R blockade on the progressive development of AD-related lesions and associated memory impairments has not been investigated yet. Furthermore, even if Tau pathology has a pivotal role in AD,[12,13] the relationships between A_{2A}Rs and Tau pathology have been totally overlooked.

In the present study, we explored the outcome of A_{2A}R gene deletion in the THY-Tau22 transgenic mouse model, which progressively develops hippocampal Tau pathology and spatial memory defects.[14,15] Our data demonstrate that A_{2A}R deletion normalizes memory, hippocampal plasticity and neurotransmitter imbalance, but also reduces Tau hyperphosphorylation in these transgenic animals. In addition, oral administration of a selective A_{2A}R antagonist (MSX-3) improves spatial memory and reduces Tau hyperphosphorylation in Tau mice. These findings support the concept of A_{2A}Rs as valuable targets against AD progression and pathology.

MATERIALS AND METHODS

Animals

A_{2A}R knockout animals and THY-Tau22 Tau transgenic mice have been described elsewhere.[14,15,16] Parental lines used were both on C57Bl6/J background. Experimental animals were generated by mating THY-Tau22

[1]Université de Lille, UDSL, Lille, France; [2]Inserm UMR837, Jean-Pierre Aubert Research Centre, Lille, France; [3]Inserm U1028—UMR 5292 CNRS—UCBL1, Centre of Research in Neurosciences, Lyon, France; [4]Instituto de Medicina Molecular, Faculdade de Medicina da Universidade de Lisboa, Lisboa, Portugal; [5]PharmaCenter Bonn, Pharmaceutical Institute, University of Bonn, Bonn, Germany; [6]Department of Chemistry, Faculty of Science, Sultan Qaboos University, Muscat, Oman; [7]NeuroDialyTics, Lyon, France; [8]Laboratory of Biological Psychology, Department of Psychology, KUL, Leuven, Belgium; [9]IRIBHM, Université Libre de Bruxelles, Brussels, Belgium and [10]CHRU-Lille, Faculté de Médecine, Lille, France. Correspondence: Dr D Blum, Inserm UMR837, 'Alzheimer & Tauopathies', Place de Verdun, Lille Cedex, 59045, France.
E-mail: david.blum@inserm.fr
[11]These authors share equal authorship as co-first authors.
[12]These authors share equal authorship as equal co-second authors.
Received 16 June 2014; revised 19 September 2014; accepted 6 October 2014; published online 2 December 2014

male mice with $A_{2A}^{+/-}$ female animals. F1 THY-Tau22 $A_{2A}^{+/-}$ males were then crossed with $A_{2A}^{+/-}$ females to generate F2 double-mutant animals, that is, THY-Tau22 $A_{2A}^{-/-}$ (referred as Tau $A_{2A}^{-/-}$), and related littermate controls, that is, WT $A_{2A}^{+/+}$, WT $A_{2A}^{-/-}$ and THY-Tau22 $A_{2A}^{+/+}$ (referred as Tau $A_{2A}^{+/+}$). Genotyping was realized by PCR analysis of tail DNA as described.[14,16] Mice were housed in a pathogen-free facility, 5 to 6 per cage (Techniplast cages 1284L; Lyon, France), maintained on a 12-h light/12-h dark cycle with *ad libitum* access to food and water. Body temperature was evaluated before animal sacrifice and showed no statistical differences between groups (not shown). We did not identify any differences in the mouse survival rate, regardless of the genotype. Since no overt gender differences were observed (see for instance Supplementary Figure 1), data from both males and females were analysed as a single group. All experiments were performed at 6–7 months of age, when Tau transgenic mice are known to exhibit significant Tau pathology and memory alterations.[17,18] All protocols were approved by an ethics committee (no. 342012, CEEA).

Treatment of THY-Tau22 mice with MSX-3

MSX-3 is a water-soluble prodrug of the potent and highly selective A_{2A}R antagonist MSX-2[19] that crosses the blood–brain barrier.[20] The drug was given to THY-Tau22 male mice in drinking water at a dose of 0.3 g l^{-1}. Chronic delivery at this dose achieved, in 7-month-old C57Bl6/J mice, plasma and brain concentrations of MSX-2 of about 10–20 nM (not shown), compatible with A_{2A}R blockade (K_i = ca. 8 nM). At this dose, MSX-3 alone was devoid of effects on hippocampal-dependent memory in C57Bl6/J mice (not shown). Animals were randomized according to their body weight into the following three experimental groups: WT/H_2O, THY-Tau22/H_2O and Tau/MSX-3. The MSX-3 solution was kept in bottles protected from light and changed weekly. Treatment was started at 6 months of age, an age at which Tau pathology and memory impairments are already significant in THY-Tau22 mice (see Figures 1 and 2), and was continued until 8.5–9 months of age. Body weight was measured weekly. MSX-3 consumption was assessed throughout treatment for each experimental cage, allowing to

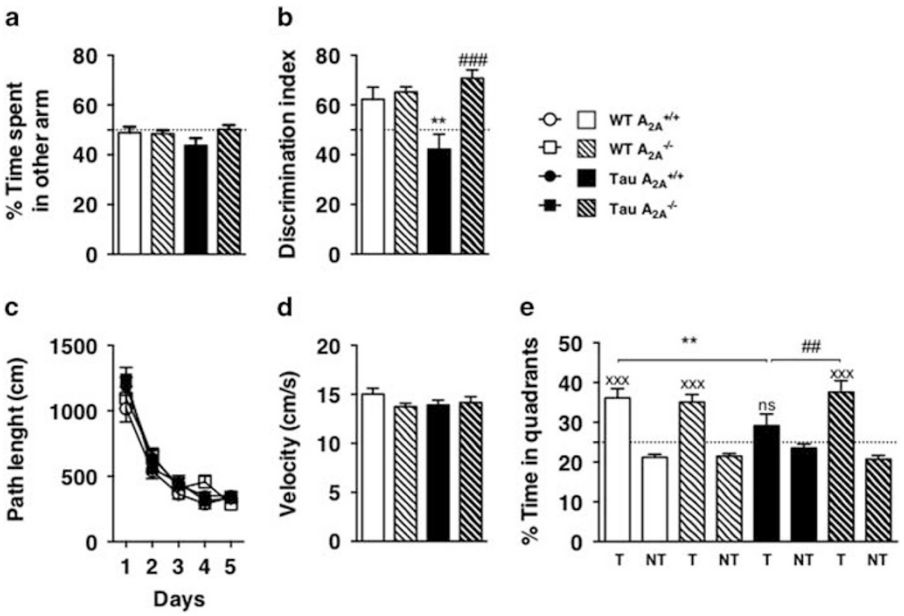

Figure 1. Adenosine A_{2A} receptor (A_{2A}R) deletion prevents behavioural impairments in Tau transgenic mice. (**a**, **b**) Effect of A_{2A}R deletion on spatial memory using Y-maze task. (**a**) During the exposure phase, all groups explored the maze equally, spending a similar amount of time in each available arm ($P > 0.05$, one-way analysis of variance (ANOVA)). (**b**) During the test phase, the discrimination index, representative of a spatial preference for the 'novel' arm, was significantly set above chance (50%) for WT $A_{2A}^{+/+}$ and WT $A_{2A}^{-/-}$ animals ($P < 0.05$ for WT $A_{2A}^{+/+}$, $P < 0.001$ for WT $A_{2A}^{-/-}$ vs 50%; Student's *t*-test). While hippocampus-dependent spontaneous spatial novelty preference was impaired in Tau $A_{2A}^{+/+}$ mice ($^{**}P < 0.01$ vs WT $A_{2A}^{+/+}$, one-way ANOVA), Tau $A_{2A}^{-/-}$ mice exhibited a normalized preference for the 'novel' arm ($^{###}P < 0.001$ vs Tau $A_{2A}^{+/+}$, one-way ANOVA), indicating that A_{2A} deletion prevented memory alterations in Tau transgenic mice. $N = 7$–11 per group. (**c**–**e**) Effect of A_{2A}R deletion on spatial memory using the Morris water maze. (**c**) Learning was found to be similar for all genotypes, as indicated by the equivalent path length needed to find the hidden platform ($P > 0.05$, two-way ANOVA). (**d**) All genotypes exhibited a comparable velocity in the maze, suggesting no motor deficits ($P > 0.05$, one-way ANOVA). (**e**) Spatial memory was assessed 72 h after the last day of learning. Results represent the percentage of time spent in the target (T) vs non-target (NT) quadrants. Wild-type (WT) animals (both $A_{2A}^{+/+}$ and $A_{2A}^{-/-}$) spent significantly more time in the T quadrant, indicative of a preserved spatial memory. While Tau $A_{2A}^{+/+}$ mice displayed memory deficits as underlined by their lack of preference for the T quadrant, Tau $A_{2A}^{-/-}$ mice behaved as non-transgenic animals, suggesting a rescue of Tau-related memory impairments by A_{2A}R deletion. $^{xxx}P < 0.001$, NT vs T (Student's *t*-test); $^{**}P < 0.01$, Tau $A_{2A}^{+/+}$ vs WT $A_{2A}^{+/+}$, and $^{\#\#}P < 0.01$, Tau $A_{2A}^{+/+}$ vs Tau $A_{2A}^{-/-}$ (one-way ANOVA); $N = 19$–24 per group. Results are expressed as mean ± s.e.m.

Figure 2. Adenosine A_{2A} receptor (A_{2A}R) deletion reduces hippocampal Tau phosphorylation and impacts Tau kinases in THY-Tau22 mice. (**a**) Representative two-dimensional profile of total human Tau in Tau $A_{2A}^{+/+}$ (top) vs Tau $A_{2A}^{-/-}$ (bottom) mice, showing a reduced amount of Tau acidic species in Tau $A_{2A}^{-/-}$ animals (arrow; Total Tau C-ter antibody). (**b**) Quantification of Tau phosphorylation on Thr212/Ser214, Ser262, Thr181, Ser404 and Ser214 epitopes, as well as dephosphorylated Tau (Tau1) in Tau $A_{2A}^{+/+}$ and Tau $A_{2A}^{-/-}$ mice ($^{\#}P < 0.05$ vs Tau $A_{2A}^{-/-}$, $N = 6$–7 per group, Student's *t*-test). Results are expressed as a percentage of Tau $A_{2A}^{+/+}$ ± s.e.m. (**c**) Representative western blots of sarkosyl-soluble (S) and -insoluble (I) hippocampal Tau species of Tau $A_{2A}^{+/+}$ (top) and Tau $A_{2A}^{-/-}$ (bottom) mice, showing no overt difference between the two genotypes (Total Tau C-ter antibody). T shows the total amounts of Tau in non-fractionated samples. Quantification of insoluble Tau species is represented in the graph below ($N = 5$ per group). (**d**) Quantification of the Tau kinase changes (GSK3β, AMPK, Erk, P38, JNK and cdk5 and its regulator p35/p25), as well as of the catalytic subunit of its main phosphatase PP2A ($^{\#}P < 0.05$ and $^{\#\#}P < 0.01$ vs Tau $A_{2A}^{-/-}$, $N = 6$–7 per group, Student's *t*-test). Results are expressed as a percentage of Tau $A_{2A}^{+/+}$ ± s.e.m.

estimate the average consumption per mice. Body temperature was evaluated at completion of the protocol before the Y-maze task.

Behavioural evaluation

Exploratory test. Open-field exploration was examined using a 50 cm × 50 cm arena. Each mouse was placed in the arena for 10 min. Movements were recorded using EthoVision video tracking equipment and software (Noldus Bv, Wageningen, The Netherlands). Total path length was measured as an index of mouse locomotion.

Rotarod test. Motor coordination and equilibrium were tested on an accelerating rotarod (MED Associates Inc., St Albans, VT, USA). Mice were

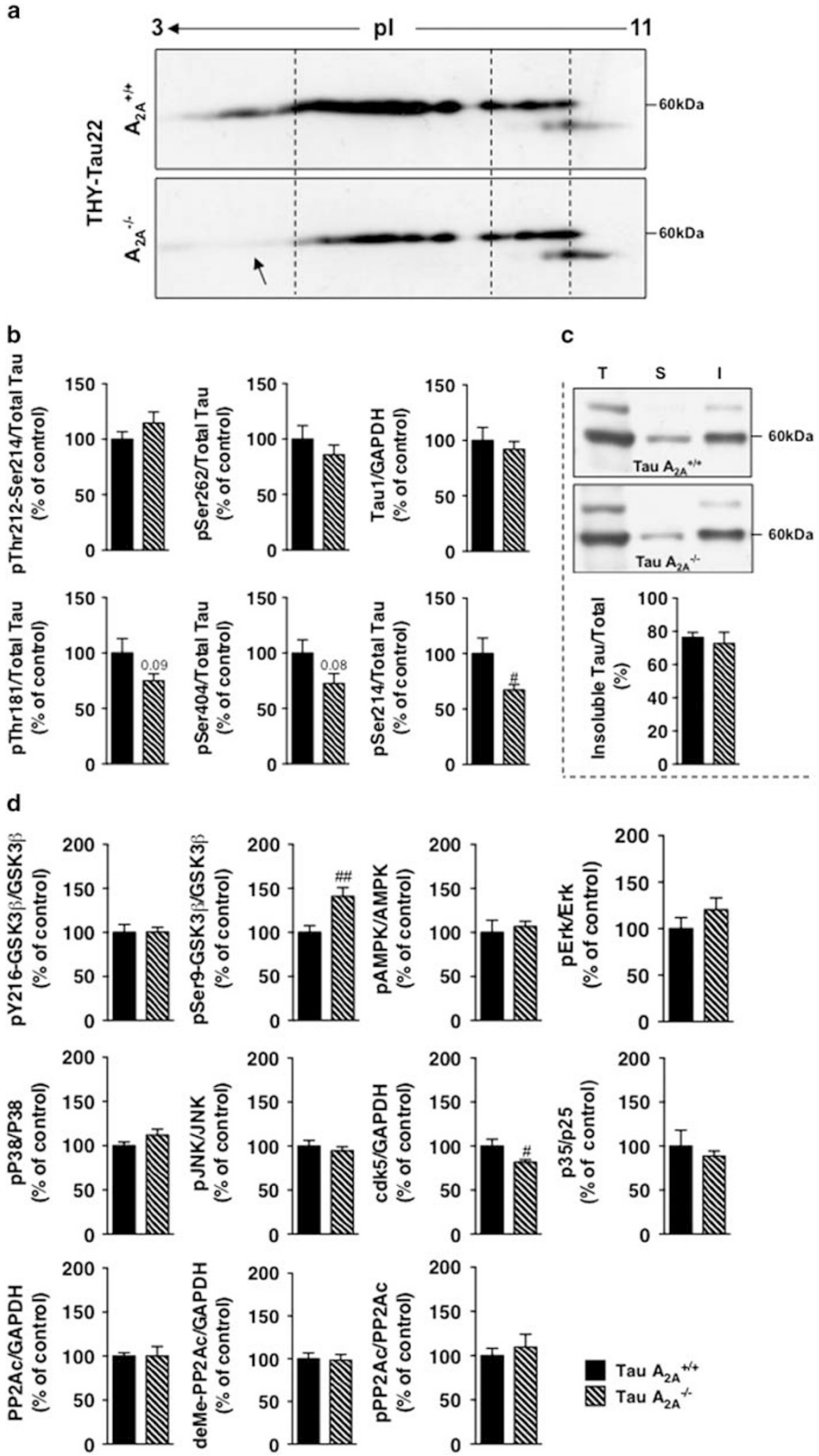

placed on the rod with their head directed against the direction of the rotation so that the animal had to progress forward to maintain its balance. Mice were first trained on a constant speed (4 r.p.m., 2 min) before starting with four test trials (intertrial interval, 10 min). During these trials, mice had to balance on the rotating rod that accelerated from 4 to 40 r.p.m. within 5 min. The latency until the mice fell from the rotating rod was recorded, up to a maximum of 5 min.

Anxiety test. The elevated plus maze was used to investigate anxiety-related behaviour. The apparatus consisted of a plus-shaped maze with two closed and two open arms (5 cm wide). Mice were placed at the centre of the maze with their face in the direction of a closed arm, and were allowed to explore freely for 10 min. Five infrared beam detectors, connected to a PC activity logger, recorded the behaviour of the mice. Percentage of time spent in the open arms was recorded.

Y-maze test. Short-term spatial memory was assessed in a spontaneous novelty-based spatial preference Y-maze test as described.[21] Each arm of the Y-maze was 22 cm long, 6.4 cm wide, with 15-cm-high opaque walls. Different extramaze cues were placed on the surrounding walls. Sawdust was placed in the maze during the experiments and mixed between each phase. Allocation of arms was counterbalanced within each group. During the exposure phase, mice were placed at the end of the 'start' arm and were allowed to explore the 'start' arm and the 'other' arm for 5 min (beginning from the time the mouse first left the start arm). Access to the third arm of the maze ('novel' arm) was blocked by an opaque door. The mouse was then removed from the maze and returned to its home cage for 2 min. In the test phase the mouse was placed again in the 'start' arm of the maze, the door of the 'novel' arm was removed and the mouse was allowed to explore the maze for 1 min (from the time the mouse first left the start arm). The amount of time the mouse spent in each arm of the maze was recorded during both exposure and test phases using EthovisionXT (Noldus Information Technology, Wageningen, The Netherlands). For the exposure phase, we calculated the percentage of time spent in the 'other' arm vs the 'start' arm. For the test phase, a discrimination index [novel arm/(novel+other arm)] × 100 was calculated.

Morris water maze. Spatial memory abilities were evaluated in the standard hidden platform (PF) acquisition and retention version of the water maze, as we previously described.[3] A 100-cm circular pool was filled with water, opacified with non-toxic white paint (Viewpoint, Lyon, France) and kept at 21 °C. A 10-cm round PF was hidden 1 cm beneath the surface of the water at a fixed position. Four positions around the edge of the tank were arbitrarily designated 1, 2, 3 and 4, thus dividing the tank into four quadrants (clockwise): target (hidden PF contained), adjacent 1, opposite and adjacent 2.

During the learning procedure, mice were tested during the light phase between 08:00 and 18:00 hours. Each mouse was given four swimming trials per day (20-min intertrial interval) for five consecutive days. The start position (1, 2, 3 or 4) was pseudo-randomized across trials. A trial consisted of placing the mouse into the water facing the outer edge of the pool in one of the virtual quadrants and allowing it to escape to the hidden PF. A trial terminated when the animal reached the PF, where it was allowed to remain for 15 s. If the animal failed to find the target before 120 s, it was manually guided to the PF, where it was allowed to stay for 15 s. After completion of a trial, mice were removed from the pool and placed back to their home cages beneath heat lamps in order to reduce the loss of temperature. Time required to locate the hidden escape PF (escape latency) and distance travelled to the hidden escape PF (path length) was recorded using the Ethovision XT tracking system (Noldus, Wageningen, The Netherlands). Swimming speed (that is, velocity, as a measure of possible motor defects that could interfere with their ability to perform in this task) was also measured. Seventy-two hours following the acquisition phase, a probe trial was conducted. During this probe trial (60 s), the PF was removed and the search pattern of the mice was tracked again. Proportion of time spent in the target quadrant vs averaged non-target quadrants was determined.

Biochemical analyses

Mice used for biochemical evaluations and mRNA studies were quickly killed by decapitation, as anaesthesia promotes Tau hyperphosphorylation.[22] Brains were removed and hippocampi were dissected out using a coronal acrylic slicer (Delta Microscopies, Mauressac, France) at 4 °C and stored at − 80 °C until use.

For all biochemical experiments, tissue was homogenized in 200 µl Tris buffer (pH 7.4) containing 10% sucrose and protease inhibitors (Complete; Roche Diagnostics, Meylan, France), sonicated and kept at − 80 °C until use. Protein amounts were evaluated using the BCA assay (Pierce, Rockford, IL, USA).

Bi-dimensional electrophoresis experiments were performed as previously described.[23] Briefly, lysates were precipitated with methanol/chloroform. Fifteen micrograms of proteins were dissolved in 2D buffer (7 M urea, 2 M thiourea, 4% CHAPS and 0.6% pharmalytes). Lysates were loaded on immobilized pH gradient strip 3–11 ReadyStrip (Amersham GE, Velizy-Villacoublay, France) and isoelectrofocused with the Protean IEF cell (Amersham GE) according to the manufacturer's instructions. The strips were layered onto a 4–12% Bis–Tris poly-acrylamide gel. Membranes were incubated with anti-total Tau antibody (Cter).

For sarkosyl-soluble/insoluble protein preparations, hippocampi were homogenized by sonication in a lysis buffer containing 10 mM Tris-HCl, pH 7.4, 0.32 M sucrose, 800 mM NaCl and 1 mM EGTA with protease inhibitors (Complete w/o EDTA, Roche Diagnostics), and centrifuged at 12 000 *g* for 10 min at 4 °C.[24] The supernatant incubated 1 h in 1% sarkosyl (*N*-laurylsarkosine sodium salt, Sigma, Saint-Quentin-Fallavier, France) at room temperature was then centrifuged at 100 000 *g* for 1 h at 4 °C, thus forming the supernatant and pellet containing sarkosyl-soluble and -insoluble Tau species, respectively. Sarkosyl-insoluble proteins were directly resuspended in LDS 2 × and sarkosyl-soluble samples were mixed with LDS 2 ×, supplemented with reducing agents (Invitrogen, Saint Aubin, France). Sarkosyl-soluble and -insoluble samples were loaded onto NuPage Novex (Invitrogen) gels at a ratio of 1:2 (v:v).

For western blots, proteins were diluted with LDS 2 × supplemented with reducing agents (Invitrogen) and then separated on NuPage Novex gels (Invitrogen). Proteins were transferred to nitrocellulose membranes, which were then blocked (5% non-fat dry milk or 5% bovine serum albumin in TNT:Tris-HCl 15 mM, pH 8, NaCl 140 mM, 0.05% Tween) and incubated with primary and secondary antibodies. Signals were visualized using chemiluminescence kits (ECLTM, Amersham Velizy-Villacoublay, Villacoublay, France) and a LAS3000 imaging system (Fujifilm, Tokyo, Japan). Total proteins were quantified vs glycéraldéhyde-3-phosphate déshydrogénase. Phosphorylated proteins were quantified vs total counterpart. Quantifications were performed using ImageJ software. All primary antibodies used are described in Table 1.

mRNA extraction and quantitative real-time reverse transcription (RT)-PCR analysis

Total RNA was extracted from hippocampi and purified using the RNeasy Lipid Tissue Mini Kit (Qiagen, Courtaboeuf, France). One microgram of total RNA was reverse-transcribed using the Applied Biosystems (Saint-Aubin, France) High-Capacity cDNA reverse transcription kit. Quantitative real-time reverse transcriptase-PCR analysis was performed on an Applied Biosystems Prism 7900 System using Power SYBR Green PCR Master Mix. The thermal cycler conditions were as follows: hold for 10 min at 95 °C, followed by 45 cycles of a two-step PCR consisting of a 95-°C step for 15 s followed by a 60-°C step for 25 s. Sequences of the primer used are given in Table 2. Cyclophilin A was used as internal control. Amplifications were carried out in triplicate and the relative expression of target genes was determined by the ΔΔCT method.

ELISA analysis

Hippocampal tissues were homogenized in RIPA buffer (Tris HCl 25 mM, NaCl 150 mM, NP40 1%, sodium deoxycholate 1%, SDS 0.1%, pH 7.6). The resulting lysates were sonicated and incubated for 1 h at 4 °C under agitation before centrifugation (12 000 *g*, 4 °C, 15 min). Supernatants were collected and protein amounts evaluated using the BCA assay (Pierce). CCL3, CCL4 and CCL5 levels were quantified using commercially available ELISA assays (R&D Systems, Abingdon, UK) after loading 300 µg of proteins in 50 µl volume.

Immunohistochemistry

GFAP immunohistochemistry was performed as previously described[21] using 40 µm floating brain sections from paraformaldehyde-perfused brains of the different experimental groups. Quantification of the GFAP staining intensity was performed using Image J Software (Scion Image, Bethesda, MD, USA).

Table 1. Antibodies used in this study

Name	*Abbreviation*	*Epitope*	*Type*	*Origin*	*Provider*	*WB*
Tau						
Anti-phospho-MAPT (pSer214)	PS214	pS214	Poly	Rabbit	Sigma	1/1000
Anti-PHF, clone AT100	AT100	pT212, pS214	Mono	Mouse	Thermo Scientific	1/1000
Anti-phospho-MAPT (pThr181)	AT270	pT181	Mono	Mouse	Thermo Scientific	1/1000
Anti-phospho-MAPT (pSer404)	PS404	pS404	Poly	Rabbit	Invitrogen	1/10 000
Anti-phospho-MAPT (pSer262)	PS262	pS262	Poly	Rabbit	Invitrogen	1/1000
Anti-Tau-1, clone PC1C6	Tau1	Non-phospho-S195,198, 199, 202	Mono	Mouse	Millipore	1/2000
Anti-total Tau	Cter	Cter last 15 aa of COOH terminus	Poly	Rabbit	Home-made	1/2000
Others						
CDK5 (C-8)	CDK5	CDK5 COOH terminus	Poly	Rabbit	Santa Cruz Biotechnology	1/1000
Phospho-p44/42 MAPK (Erk1/2)	P-ERK	pT202, pY204	Mono	Mouse	Cell Signaling Technology	1/1000
p44/42 MAPK (Erk 1/2) (3A7)	ERK	Mouse Erk 1/2	Mono	Mouse	Cell Signaling Technology	1/1000
Phospho-GSK-3β (Ser9)	P-GSK3β (S9)	pS9	Poly	Rabbit	Cell Signaling Technology	1/1000
Phospho-GSK3 (Tyr279/Tyr216) clone 5G-2F	P-GSK3β (Y216)	pY279/Y216	Mono	Mouse	Millipore	1/1000
GSK-3α/β (011-A)	GSK3	Mouse GSK3β1-420	Mono	Mouse	Santa Cruz Biotechnology	1/2000
Phospho-AMPKα (Thr172)	P-AMPK	pT172	Poly	Rabbit	Cell Signaling Technology	1/1000
AMPKα	AMPK	Human AMPKα amino-terminal region	Poly	Rabbit	Cell Signaling Technology	1/1000
P35 (C-19)	P35	Human P35 COOH terminus	Poly	Rabbit	Santa Cruz Biotechnology	1/1000
Phospho-p38 MAPK (Thr180/Tyr182)	P-P38	pT180/pT182	Poly	Rabbit	Cell Signaling Technology	1/1000
P38 MAPK	P38	Human p38	Poly	Rabbit	Cell Signaling Technology	1/1000
Phospho-JNK (Thr183/Tyr185)	P-JNK	pT183/pY185	Poly	Rabbit	Cell Signaling Technology	1/1000
JNK	JNK	Mouse JNK	Poly	Rabbit	Cell Signaling Technology	1/1000
Anti-PP2A, C subunit, clone 1D6	PP2A C	Human PP2A C subunit 295-309	Mono	Mouse	Millipore	1/2000
Demethylated-PP2A, C clone 4B7	deMe-PP2A	Unmethylated C-terminal region	Mono	Mouse	Santa Cruz Biotechnology	1/1000
Phospho-PP2A (Tyr307)	P-PP2A	pY307	Poly	Rabbit	Abcam	1/1000
GAPDH	GAPDH	Human GAPDH FL1-335	Poly	Rabbit	Santa Cruz Biotechnology	1/10 000

Abbreviations: AMPK, 5' AMP-activated protein kinase; GAPDH, glycéraldéhyde-3-phosphate déshydrogénase; GSK3β, glycogen synthase kinase 3β; JNK, c-Jun N-terminal kinase; MAPT, microtubule-associated protein tau; Mono, monoclonal; PHF, paired-helical filaments; Poly, polyclonal; WB, dilution used in western blotting.

Table 2. Primer sequences used in this study

Name	*Accession number*	*Primer FW (5′–3′)*	*Primer R (5′–3′)*	*Amplicon size*
CD68	NM_009853.1	GACCTACATCAGAGCCCGAGT	CGCCATGAATGTCCACTG	95
GFAP	NM_001131020.1	CGCGAACAGGAAGAGCGCCA	GTGGCGGGCCATCTCCTCCT	104
CCL3	NM_011337.2	TGCCCTTGCTGTTCTTCTCT	GTGGAATCTTCCGGCTGTAG	112
CCL4	NM_013652.2	GCCCTCTCTCTCCTCTTGCT	GAGGGTCAGAGCCCATTG	72
CCL5	NM_013653.3	CTCACTGCAGCCGCCCTCTG	CCGAGCCATATGGTGAGGCAGG	51
TNFα	NM_013693.2	TGCCTATGTCTCAGCCTCTTC	GAGGCCATTTGGGAACTTCT	116
GAT1	NM_178703.4	TGTTGGTTGGACTGGAAAGG	ACGGAAGAACAGGATGATAAG	75
GAT2	NM_144512.2	GTGCCCATATCTGAGGTTGC	ATCACCACAGCTCGAGGGTA	70
GAT3	NM_172890.3	GAGCAGGGTGTGCCTATTG	GTAGGCGATGAAAGCCAGTC	62
hTau	NM_016835.4	GTACGGGTTGGGGGACAGGA	CCCGGTTCCTCAGATCCGTC	129
Cyclophilin	NM_008907.1	AGCATACAGGTCCTGGCATC	TTCACCTTCCCAAAGACCAC	126

Abbreviations: FW, forward; R, reverse.

Electrophysiological recordings

Animals were killed by cervical dislocation, decapitated, the brain rapidly removed and the hippocampi dissected in ice-cold Krebs solution composed of (mM): NaCl 124; KCl 3; NaH_2PO_4 1.25; $NaHCO_3$ 26; $MgSO_4$ 1; $CaCl_2$ 2; and glucose 10 (previously gassed with 95% O_2 and 5% CO_2, pH 7.4). Slices (400 μm thick) were obtained with a McIlwain tissue chopper, left to recover for at least 1 h in Krebs solution, and field excitatory postsynaptic potentials were recorded as previously described in the CA1 stratum radiatum.[25] Long-term depression protocol (LTD, 3 trains with 10 min interval of 2 Hz, 1,200 pulses) was adapted from Van der Jeug *et al.*,[26] recorded at 32 °C with a constant flow of 3 ml min^{-1}.

Microdialysis and neurotransmitter determinations

For microdialysis studies, mice were anaesthetized with urethane (1.62 g kg^{-1}, i.p.) and placed in a stereotaxic frame (David Kopf, Tujunga, CA, USA) with the body temperature maintained close to 37.5 °C using a heated under-blanket (Harvard Instruments, Les Ulis, France). The skull was exposed and, after drilling an appropriate hole, a homemade microdialysis probe was implanted in a randomized manner in the right or left dorsal hippocampus (coordinates relative to the bregma: AP −1.8 mm, L ±1.5 mm, V −2.4 mm below the brain surface) according to the atlas of Franklin & Paxinos. Concentric microdialysis probes were constructed from regenerated cellulose dialysis tubing (MWCO 6000 Da, 225 mm o.d., 1 mm active dialysis length) and fused-silica capillary tubing, the body of the probe being made of a 3-cm 26-G stainless steel tube. The probes were perfused at a rate of 1 μl min^{-1} with artificial cerebrospinal fluid (149 mM NaCl, 2.80 mM KCl, 1.2 mM $MgCl_2$, 1.2 mM $CaCl_2$, 2.78 mM phosphate buffer, pH 7.4). At least 2 h was allowed to elapse after microdialysis probe implantation before collection of basal samples (fractions 1, 2 and 3). Samples were collected every 5 min. Samples were stored and kept at −80 °C before analyses. At the end of the experiment, the mice were decapitated; the implanted hemisphere was removed and the placement of the cannula was verified on the frozen hemisphere.[27]

To evaluate gamma-amino butyric acid (GABA) and glutamate levels in dialysates, 5 μl of sample and 5 μl of standard solutions were derivatized at room temperature by adding 2 μl of a mixture (1:2:1 v/v/v) of (i) internal standard (10–4 mol l^{-1} cysteic acid in 0.117 mol l^{-1} perchloric acid), (ii) a

borate/NaCN solution (100:20 v/v mixture of 500 mmol l^{-1} borate buffer, pH 8.7, and 87 mmol l^{-1} NaCN in water) and (iii) a 2.925-mmol l^{-1} solution of naphthalene-2,3-dicarboxaldehyde in acetonitrile/water (50:50 v/v). The samples were then analysed for amino-acid content using an automatic capillary electrophoresis P/ACE™ MDQ system (Beckman, Brea, CA, USA) equipped with a ZETALIF laser-induced fluorescence detector (Picometrics, Labege, France). Excitation was performed using a diode laser (Oxxius, Lannion, France) at a wavelength of 410 nm, the emission wavelength being 490 nm. Separations were carried out on a 63 cm × 50 μm i.d. fused-silica capillary (Composite Metal Services, Worcester, England) with an effective length of 52 cm. Each day, before the analyses, the capillary was sequentially flushed with 0.25 mol l^{-1} NaOH (15 min), ultra-pure water (15 min) and running buffer (75 mmol l^{-1} sodium borate, pH 9.20 ± 0.02, containing 10 mmol l^{-1} HP-β-CD and 70 mmol l^{-1} SDS) (5 min). The separation conditions were an applied voltage of 25 kV, hydrodynamic sample injection (10 s at 0.6 psi) and a temperature between 41 and 43 °C. The capillary was sequentially flushed for 30 s each with 0.25 mol l^{-1} NaOH, ultra-pure water and running buffer between analyses. Electropherograms were acquired at 15 Hz using Karat 32 software.[28]

Statistics

Results are expressed as means ± s.e.m. Differences between mean values were determined using the Student's *t*-test, two-way analysis of variance (ANOVA) or one-way ANOVA, followed by a *post-hoc* Fisher's LSD test using Graphpad Prism Software. *P* values < 0.05 were considered significant.

RESULTS

A_{2A}R deletion prevents behavioural impairments in Tau transgenic mice

We evaluated the impact of A_{2A}R deletion on behavioural impairments of THY-Tau22 mice at the age of 7 months. First, we determined the effects of A_{2A}R deletion on spatial memory using Y-maze task. During the exposure phase, all groups explored the maze equally, spending a similar amount of time in the two available arms ($P > 0.05$; Figure 1a). During the test phase, we found that the discrimination index, reflecting the preference of mice for the novel arm vs the familiar arm, was significantly above chance (that is, >50%) for WT $A_{2A}^{+/+}$ ($P = 0.03$) and WT $A_{2A}^{-/-}$ ($P < 0.0001$) animals, both groups exhibiting a similar performance ($P = 0.6$, one-way ANOVA; Figure 1b). Importantly, while Tau $A_{2A}^{+/+}$ mice exhibited an impaired preference for the new arm ($P = 0.24$ when compared to chance, that is, 50%; $P = 0.0023$ in Tau $A_{2A}^{+/+}$ vs WT $A_{2A}^{+/+}$, one-way ANOVA), the discrimination index of Tau $A_{2A}^{-/-}$ animals was found to be significantly higher than that of Tau $A_{2A}^{+/+}$ mice ($P = 0.0003$ in Tau $A_{2A}^{-/-}$ vs Tau $A_{2A}^{+/+}$, one-way ANOVA; $P = 0.0015$ when compared to chance, that is, 50%; Figure 1b), indicative of an improved spatial memory.

In addition, we evaluated the impact of A_{2A}R deletion on the development of memory impairments of THY-Tau22 mice using Morris water maze. As shown in Figure 1c, following path length calculations, there was no significant difference between groups during the learning phase using two-way ANOVA analysis ($P > 0.05$). Also, neither Tau nor A_{2A} genotypes influenced animal velocity ($P > 0.05$; Figure 1d). Seventy-two hours following acquisition, a probe trial was performed. Regardless of A_{2A}R expression, WT animals exhibited a significant preference for the target quadrant (Figure 1e; WT $A_{2A}^{+/+}$: $P < 0.0001$; WT $A_{2A}^{-/-}$: $P < 0.0001$ vs non-target quadrants), with a significantly greater proportion of time spent in the former than expected by chance (that is, >25%; WT $A_{2A}^{+/+}$: 36.1 ± 2.3%, $P < 0.0001$; WT $A_{2A}^{-/-}$: 35.1 ± 1.9%, $P < 0.0001$). Therefore, in line with the Y-maze evaluation, A_{2A}R deletion itself did not impact spatial memory in WT animals. As expected, Tau $A_{2A}^{+/+}$ mice exhibited major memory impairments with no preference for the target quadrant (Figure 1e; $P > 0.05$ vs non-target quadrants; $P = 0.17$ when compared to chance, that is, 25%), as well as a significant reduction of the percentage of time spent in the latter as compared to WT animals (WT $A_{2A}^{+/+}$: 36.1 ± 2.3% vs Tau $A_{2A}^{+/+}$: 29.1 ± 2.9%, $P = 0.009$; one-way ANOVA). In sharp contrast, A_{2A}R deletion prevented memory impairments in THY-Tau22 animals. Indeed, Tau $A_{2A}^{-/-}$ mice manifested a significant preference for the target quadrant (Figure 1e, $P < 0.0001$ vs non-target quadrants) and spent a significantly greater proportion of their time in the former than expected by chance (37.6 ± 2.9%, $P = 0.0003$). Furthermore, one-way ANOVA analysis indicated that Tau $A_{2A}^{-/-}$ mice spent a higher percentage of time in the target quadrant than Tau $A_{2A}^{+/+}$ animals (37.6 ± 2.9% vs 29.1 ± 2.9%; $P = 0.002$; Figure 1e), while they exhibited a score similar to WT $A_{2A}^{+/+}$ (37.6 ± 2.9% vs 36.1 ± 2.3%; $P = 0.6$) and WT $A_{2A}^{-/-}$ groups (37.6 ± 2.9% vs 35.1 ± 1.9%; $P = 0.36$). In THY-Tau22 mice, similar beneficial effects of A_{2A}R deletion were found regardless of mice gender (Supplementary Figure 1). Altogether, these behavioural evaluations indicated that A_{2A}R deletion prevents spatial memory alterations in THY-Tau22 mice.

Of note, we also checked motor performances using open-field and rotarod tasks. We did not find significant differences in path length and latency to fall between experimental groups (Supplementary Figures 2A and B). We also analysed the impact of A_{2A}R deletion on anxiety using the elevated plus maze task. THY-Tau22 mice spent significantly more time in the open arms as compared to controls (WT: 28.7 ± 1.6% vs Tau $A_{2A}^{+/+}$: 36.7 ± 3.7%; $P = 0.04$, one-way ANOVA; Supplementary Figure 2C), whereas A_{2A}R knockout animals exhibited the opposite phenotype (WT: 28.7 ± 1.6% vs $A_{2A}^{-/-}$: 19.9 ± 2.1%, $P = 0.04$, one-way ANOVA). In the THY-Tau22 background, A_{2A}R deletion normalized the anxiety profile. Tau $A_{2A}^{-/-}$ mice spent significantly less time in the open arms than Tau $A_{2A}^{+/+}$ animals (Tau $A_{2A}^{-/-}$: 28.9 ± 2.8%, $P = 0.04$ vs Tau $A_{2A}^{+/+}$; one-way ANOVA) and exhibited a similar score to that of WT animals ($P = 0.04$ vs WT; $P = 0.95$, one-way ANOVA; Supplementary Figure 2C). A_{2A}R deletion thus appears to normalize anxiety impairments in THY-Tau22 mice.

A_{2A}R deletion reduces hippocampal Tau phosphorylation in THY-Tau22 mice

Spatio-temporal progression of Tau pathology in the AD brains correlates with the progression of cognitive symptoms.[12,13] Accordingly, progressive development of hippocampal Tau pathology parallels memory impairments in THY-Tau22 mice.[15] Therefore, we investigated whether the memory improvement seen in Tau $A_{2A}^{-/-}$ mice were related to any changes in Tau protein. In a first attempt, given the important number of phosphorylation sites on Tau (>80),[29] we performed a two-dimensional (2D) gel electrophoresis analysis to evaluate global charge changes of human Tau protein in Tau $A_{2A}^{+/+}$ vs Tau $A_{2A}^{-/-}$ animals. We observed a reduction of Tau isovariants at the acidic pH range in Tau $A_{2A}^{-/-}$ mice as compared to Tau $A_{2A}^{+/+}$ animals, suggesting a reduced Tau phosphorylation (arrow; Figure 2a).

A moderate reduction of phosphorylation was observed by sodium dodecyl sulphate-polyacrylamide gel electrophoresis at the level of several Tau phospho-epitopes. As compared to Tau $A_{2A}^{+/+}$ animals, Thr181 and Ser404 epitopes showed a trend for reduced phosphorylation in Tau $A_{2A}^{-/-}$ animals (Thr181: −24.9 ± 6.1%, $P = 0.09$; Ser404: −27.4 ± 8.8%, $P = 0.09$ vs Tau $A_{2A}^{+/+}$, Student's *t*-test) and phosphorylation on Ser214 was found to be significantly reduced (−32.9 ± 5.1% of Tau $A_{2A}^{+/+}$, $P = 0.04$, Student's *t*-test; Figure 2b and Supplementary Figure 3a). Conversely, phosphorylation on Thr212/Ser214 (AT100) and Ser262 epitopes as well as Tau1 staining, reflecting dephosphorylated Tau at Ser195/198/199/202, remained unchanged in Tau $A_{2A}^{-/-}$ vs Tau $A_{2A}^{+/+}$ animals ($P = 0.26$, $P = 0.35$ and $P = 0.56$, respectively, Student's *t*-test; Figure 2b and Supplementary Figure 3a). Noteworthy, A_{2A}R deletion did not influence transgene expression as human Tau mRNA levels remained unchanged in Tau $A_{2A}^{-/-}$ vs Tau $A_{2A}^{+/+}$ animals (not shown). Tau protein levels and proteolytic fragments, known to favour aggregation,[30] were also unaffected in both groups (not shown), suggesting that A_{2A}R deletion does not affect the stability or the degradation of human Tau proteins. Finally, to study the

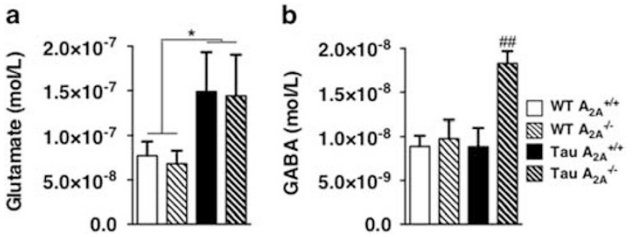

Figure 3. Adenosine A_{2A} receptor ($A_{2A}R$) deletion modulates hippocampal levels of glutamate and gamma-amino butyric acid (GABA). Glutamate (**a**) and GABA (**b**) concentrations in microdialysates recorded from the dorsal hippocampus of anaesthetized mice. The histograms represent the mean ± s.e.m. of three consecutive 5-min microdialysates following a 2-h post-implantation equilibration period ($^{*}P < 0.05$ using two-way analysis of variance (ANOVA); $^{\#\#}P < 0.01$ in Tau $A_{2A}^{-/-}$ vs Tau $A_{2A}^{+/+}$, $N = 6$–9 per group, one-way ANOVA).

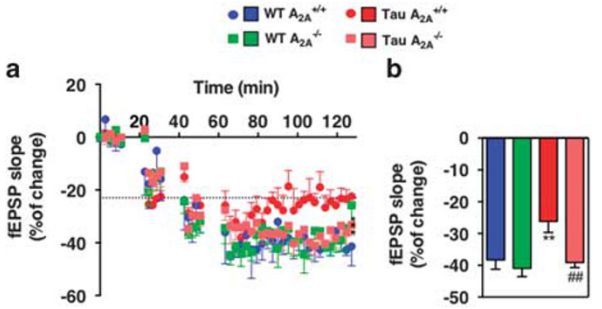

Figure 4. Adenosine A_{2A} receptor ($A_{2A}R$) deletion rescues long-term depression (LTD) deficits in THY-Tau22 transgenic mice. (**a**) Plots of the field excitatory postsynaptic potential (fEPSP) slope variation over time after induction of LTD in hippocampal slices. While Tau $A_{2A}^{+/+}$ mice displayed an impaired LTD as compared to WT ($A_{2A}^{+/+}$ or $A_{2A}^{-/-}$) animals, slices from Tau $A_{2A}^{-/-}$ animals exhibited LTD similar to control animals, suggesting that A_{2A} deletion rescues LTD in Tau mice. (**b**) Quantification of the percentage of variation of the fEPSP slope during the LTD maintenance phase, 60 min after induction ($^{**}P < 0.01$ in Tau $A_{2A}^{+/+}$ vs WT $A_{2A}^{+/+}$; $^{\#\#}P < 0.01$ in Tau $A_{2A}^{-/-}$ vs Tau $A_{2A}^{+/+}$; $N = 4$–7 per group, one-way analysis of variance).

impact of the $A_{2A}R$ knockout on Tau aggregation, biochemical fractionation was performed and sarkosyl-soluble/insoluble fractions analysed. The amount of sarkosyl-insoluble Tau remained similar in Tau $A_{2A}^{+/+}$ and Tau $A_{2A}^{-/-}$ mice ($P > 0.05$; Figure 2c).

$A_{2A}R$ deletion and kinase/phosphatase balance in THY-Tau22 mice

Tau phosphorylation is under the tight control of a kinase/phosphatase balance. More than 30 different kinases are able to phosphorylate Tau.[29] We thus evaluated the impact of $A_{2A}R$ deletion on activation of major Tau kinases, namely GSK3β, AMPK, p42/44 MAPK (Erk), p38 MAPK, JNK and Cdk5. As shown in Figure 2d and Supplementary Figure 3b, we observed that in THY-Tau22 mice $A_{2A}R$ deletion led to a significant increase of GSK3β phosphorylation at the Ser9 inactivating epitope (+40.8 ± 10.0% of Tau $A_{2A}^{+/+}$ mice; $P = 0.009$, Student's *t*-test), as well as to a mild but significant reduction of Cdk5 immunoreactivity (−18.4 ± 2.9% of Tau $A_{2A}^{+/+}$ mice; $P = 0.04$, Student's *t*-test) without any change in the level of its pathological activator p25. Conversely, phosphorylation of AMPK, Erk, p38 and JNK remained unchanged in Tau $A_{2A}^{-/-}$ mice. In addition, we addressed expression, demethylation and Y307 phosphorylation of the catalytic subunit of PP2A (PP2Ac), the main Tau phosphatase. Results showed that PP2Ac remained unaffected by $A_{2A}R$ knockout in THY-Tau22 animals (Figure 2d and Supplementary Figure 3b). The reduced Tau phosphorylation seen in Tau $A_{2A}^{-/-}$ mice thus appears to be likely associated to changes in GSK3β and cdk5 kinases.

$A_{2A}R$ deletion modulates hippocampal neuro-inflammation in THY-Tau22 mice

Tau transgenic models have been previously shown to exhibit hippocampal neuro-inflammation, progressing along the development of hippocampal Tau pathology and behavioural alterations.[3,31] Of interest, neuro-inflammation favours Tau hyperphosphorylation[32] and memory dysfunctions[33] and $A_{2A}R$ blockade has been suggested to mitigate neuroinflammatory processes.[6,34] These observations prompted us to investigate the effects of $A_{2A}R$ deletion on the neuro-inflammatory markers previously found to be upregulated in Tau transgenic mice.[3] As expected, we found that mRNA expression of microglial (CD68) and astroglial (GFAP) markers as well as of several pro-inflammatory cytokines (CCl3, CCl4, CCl5 and TNFα) were significantly upregulated in the hippocampus of Tau $A_{2A}^{+/+}$ animals, with most of them significantly reduced in Tau $A_{2A}^{-/-}$ mice (CD68: −18.8 ± 6.9%, $P = 0.03$; GFAP: −38.1 ± 4.6%, $P = 0.0004$; TNFα: −34.3 ± 7.5%, $P = 0.0004$; CCl3: −33.0 ± 11.5%, $P = 0.02$; and CCl5: −29.3 ± 10.1%, $P = 0.02$ vs Tau $A_{2A}^{+/+}$, one-way ANOVA; Supplementary Figure 4B). Using immunohistochemistry and ELISA, we confirmed that $A_{2A}R$ deletion normalized GFAP expression and CCl3 levels in Tau mice (Supplementary Figures 4B and C). In WT animals, $A_{2A}R$ deletion itself had no significant effect on the levels of all markers studied.

$A_{2A}R$ deletion modulates hippocampal levels of glutamate and GABA

$A_{2A}Rs$ regulate neuronal pre-synaptic release as well as astrocyte-based reuptake of glutamate and GABA.[6,35,36] THY-Tau22 mice exhibit higher hippocampal glutamate levels compared to WT animals, regardless of the $A_{2A}R$ genotype ($P = 0.021$; two-way ANOVA; Figure 3a). Surprisingly, hippocampal GABA levels were found to be significantly upregulated in the hippocampus of Tau $A_{2A}^{-/-}$ animals, reaching 206 ± 16% of Tau $A_{2A}^{+/+}$ ($P = 0.003$ using one-way ANOVA; Figure 3b). Subsequently, glutamate/GABA ratio was found to be increased in Tau $A_{2A}^{+/+}$ as compared to WT animals (WT $A_{2A}^{+/+}$: 7.3 ± 1.2 vs Tau $A_{2A}^{+/+}$:13.9 ± 2.8, $P = 0.05$, one-way ANOVA) while normalized to control levels in Tau $A_{2A}^{-/-}$ mice (8.4 ± 2.6, $P = 0.75$ vs WT $A_{2A}^{+/+}$). Hippocampal mRNA levels for the GABA transporters (GATs) 1, 2 and 3 were significantly increased in Tau $A_{2A}^{+/+}$ mice, whereas both GAT-2 and GAT-3 expression returned to control levels in Tau $A_{2A}^{-/-}$ animals (Supplementary Figure 5).

$A_{2A}R$ deletion rescues LTD deficits in THY-Tau22 transgenic mice

We previously demonstrated that impaired hippocampal-dependent learning and memory in THY-Tau22 transgenic mice was associated with attenuated long-term depression.[26] Slices from WT animals developed a robust and similar LTD regardless of $A_{2A}R$ expression (WT $A_{2A}^{-/-}$ vs WT $A_{2A}^{+/+}$, $P > 0.05$; two-way ANOVA; Figure 4a). As expected, Tau $A_{2A}^{+/+}$ mice exhibited an impaired LTD maintenance as compared to WT $A_{2A}^{+/+}$ animals ($P < 0.001$ vs WT $A_{2A}^{+/+}$, two-way ANOVA; Figure 4a and b), with a significant reduction, reaching 31.6 ± 3.5% of controls ($P = 0.008$ vs WT $A_{2A}^{+/+}$, one-way ANOVA; Figure 4b). In contrast, LTD remained unaffected in Tau $A_{2A}^{-/-}$ mice ($P < 0.001$ vs Tau $A_{2A}^{+/+}$, two-way ANOVA; Figure 4a), being similar to WT animals ($P = 0.82$, Figure 4b).

Beneficial effects of $A_{2A}R$-based therapy using the selective antagonist MSX-3 in Tau transgenic mice

We explored the effect of MSX-3, a water-soluble prodrug of MSX-2, which is a potent and highly selective $A_{2A}R$ antagonist.[19] THY-Tau22 mice received MSX-3 through drinking water (0.3 g l^{-1}) starting at 6 until 8.5–9 months of age. At completion of the

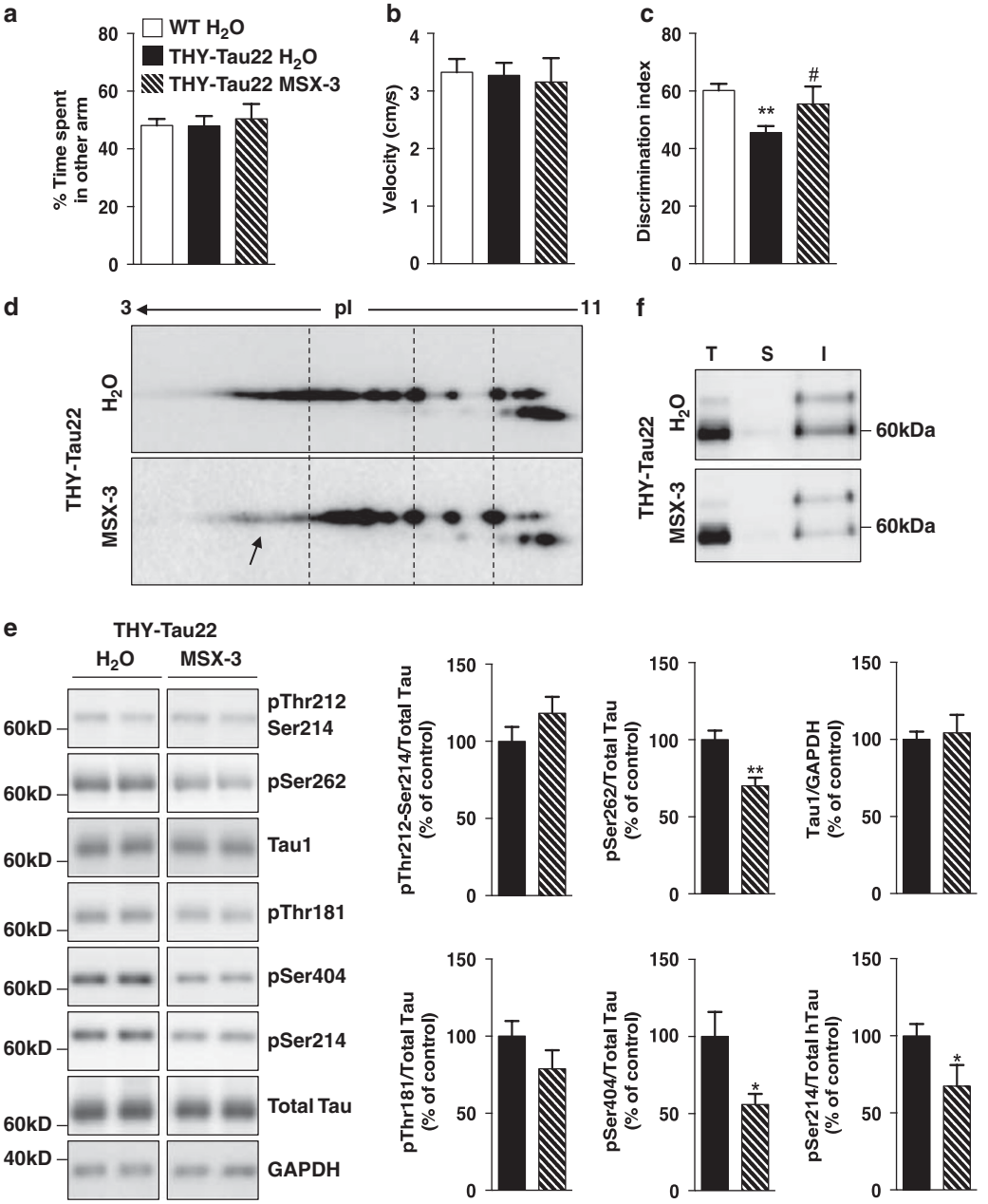

Figure 5. The specific A$_{2A}$ receptor antagonist MSX-3 improves spatial memory and reduces Tau hyperphosphorylation in THY-Tau22 mice. MSX-3 treatment started at 6 months, an age at which Tau pathology and memory impairments are already significant (see Figures 1 and 2) until 8.5–9 months. (**a–c**) Effect of MSX-3 on the spatial memory of THY-Tau22 mice using Y-maze task. During the exposure phase (**a**), all groups explored the maze equally, spending a similar amount of time in each available arm ($P > 0.05$, one-way analysis of variance (ANOVA)). All genotypes exhibited a comparable velocity in the maze (**b**; $P > 0.05$, one-way ANOVA). During the test phase (**c**), while hippocampus-dependent spontaneous spatial novelty preference was impaired in Tau/H$_2$O mice (*$P < 0.05$ vs WT, one-way ANOVA), Tau mice treated with MSX-3 exhibited a normalized preference for the 'novel' arm ($^{\#}P < 0.001$ vs Tau/H$_2$O, one-way ANOVA; $N = 9$–15 per group). (**d**) Representative two-dimensional profile of total human Tau protein in Tau/H$_2$O (top) vs Tau/MSX-3 (bottom) mice, showing a reduced amount of Tau acidic species in Tau animals treated with the adenosine A$_{2A}$ receptor antagonist (arrow; Total Tau C-ter antibody). (**e**) Tau phosphorylation on Thr212/Ser214, Ser262, Thr181, Ser404 and Ser214 epitopes, as well as dephosphorylated Tau (Tau1) in Tau/H$_2$O and Tau/MSX-3 mice (*$P < 0.05$ and **$P < 0.01$ vs Tau, $N = 6$–8 per group, Student's *t*-test). Results are expressed as a percentage of Tau/H$_2$O ± s.e.m. (**f**) Representative western blots of sarkosyl-soluble (S) and -insoluble (I) hippocampal Tau species of Tau/H$_2$O (top) and Tau/MSX-3 (bottom) mice, showing no overt difference between the two groups (Total Tau C-ter antibody).

experiment, body weight gain was not different between water- and MSX3-treated Tau animals (Tau/H$_2$O: 120.1 ± 1.4% of their initial body weight; Tau/MSX-3: 122.9 ± 1.1% of their initial body weight; $P = 0.13$ vs water consumers). Body temperature was also similar in all experimental groups (not shown). Mice consumed on average 4.7 ± 0.3 ml of the MSX-3 solution every day, corresponding to an average daily intake of 1.4 mg of the antagonist.

Spatial memory was evaluated using the Y-maze task. During the exposure phase, all groups spent a similar amount of time in the two available arms ($P > 0.05$; Figure 5a). During the test phase,

the discrimination index was significantly impaired in Tau mice treated with water ($P = 0.0022$ in Tau/H_2O vs WT/H_2O, one-way ANOVA; Figure 5c). Tau/MSX-3 animals exhibited an index higher than that of Tau/H_2O mice ($P = 0.05$ in Tau/MSX-3 vs Tau/H_2O, one-way ANOVA; Figure 5c) and similar to control animals (Tau/MSX-3 vs WT/H_2O, one-way ANOVA; $P = 0.36$), indicative of an improved spatial memory.

We then investigated whether these memory improvements were related to changes of Tau protein. Using two-dimensional (2D) gel electrophoresis analysis, we observed a reduction of Tau isovariants at the acidic pH range in Tau/MSX-3 mice as compared to Tau/H_2O animals, suggesting a reduced Tau phosphorylation (arrow; Figure 5d). Accordingly, we observed a reduction of Tau phosphorylation at several Tau phospho-epitopes using sodium dodecyl sulphate-polyacrylamide gel electrophoresis. As compared to Tau/H_2O animals, we found a significantly reduced phosphorylation at Ser262, Ser404 and Ser214 epitopes in Tau/MSX-3 vs Tau/H_2O animals (Figure 5e). Phosphorylation at Thr212/Ser214 (AT100) and Thr181 epitopes as well as Tau1 staining remained unchanged. MSX-3 treatment did not affect total Tau protein levels (Figure 5e) nor Tau proteolytic fragments (not shown). Finally, the MSX-3 effect on Tau aggregation was evaluated using biochemical fractionation. The amount of sarkosyl-insoluble Tau remained similar in Tau/H_2O and Tau/MSX-3 animals (Figure 5f).

DISCUSSION

The present study provides the first evidence that $A_{2A}R$ deletion is sufficient to prevent memory defects, hippocampal plasticity impairments as well as Tau hyperphosphorylation, in a mouse model of AD. Accordingly, our data also demonstrate that treatment with a specific $A_{2A}R$ antagonist, starting from a symptomatic stage, improves spatial memory and reduces Tau hyperphosphorylation in THY-Tau22 mice.

The role of $A_{2A}Rs$ in AD is ill-defined. Previous studies demonstrated a significant $A_{2A}R$ upsurge in the brain of AD patients, visible at early Braak stages.[37] Consistent with the view that such $A_{2A}R$ dysfunction is detrimental towards hippocampal function,[25] epidemiological and experimental studies have shown that the consumption of caffeine, a non-selective $A_{2A}R$ antagonist, reduces AD risk and mitigates AD lesions.[1,2,3] However, the specific relationship between $A_{2A}Rs$ and AD has been overlooked. While recent findings suggested that genetic and pharmacological $A_{2A}R$ blockade mitigates acute Aβ synaptotoxicity in mice,[11] the impact of $A_{2A}R$ modulation on the pathophysiological progression of AD hallmarks, including specific lesions, remained totally unknown so far.

In the present study, we demonstrate that $A_{2A}R$ deletion significantly prevents the development of spatial memory deficits in THY-Tau22 transgenic mice, using Y-maze and Morris water maze tasks. $A_{2A}R$ deletion itself does not lead to any learning and memory changes in WT animals. This is consistent with previous studies showing that, unlike working memory, global or forebrain-specific $A_{2A}R$ deletion spares spatial reference memory in mice.[38,39] Overall, our results are in agreement with previous data showing that A_{2A} receptor blockade is pro-cognitive in various conditions leading to memory decline, such as ageing,[40] chronic stress,[25] β-amyloid acute toxicity[11] or traumatic brain injury.[41] Importantly, MSX-3 treatment rescued hippocampal-dependent memory in Tau mice even after onset of the pathology. This supports the idea that A_{2A} receptor blockade is efficient not only to prevent but also to revert deficits in our model of AD-like Tau pathology. Accordingly, pharmacological A_{2A} receptor blockade was shown to revert memory deficits in a chronic stress model induced by maternal separation.[25]

Tau hyperphosphorylation has been associated to cognitive impairments in several dementing disorders[29] as well as in various experimental models.[17,42] Obviously, Tau-related memory impairments are dissociated from Tau aggregation.[3,24,43] Our present results demonstrate that $A_{2A}R$ deletion or blockade by MSX-3 promotes a moderate but significant reduction of Tau hyperphosphorylation as notably seen using 2D electrophoresis. This occurs while Tau aggregation remains unchanged, as supported by unmodified AT100 immunoreactivity and sarkosyl-insoluble Tau. This suggests that the observed memory improvements following $A_{2A}R$ deletion or pharmacological blockade are likely related, at least in part, to changes in Tau phosphorylation status. Interestingly, the effects of $A_{2A}R$ deletion on Tau pathology are distinct from those observed following chronic caffeine intake in the same mouse model.[3] Indeed, Tau epitopes found changed in the present study (essentially pSer214) are different from those found modulated by caffeine (AT100, Tau1). Moreover, in contrast to caffeine, $A_{2A}R$ deletion does not influence the amount of Tau proteolytic fragments.[3] Taken together, these data support that regulation of Tau by caffeine is likely resulting from a broader range of action than only inhibition of $A_{2A}R$ activity.

Tau phosphorylation is under the control of phosphatases, essentially PP2A, and a number of distinct kinases (>30).[29] Here, we found that the deletion of $A_{2A}R$ did not affect the expression, methylation and phosphorylation of PP2A in Tau mice. Rather, our data show that $A_{2A}R$ deletion increases the levels of pSer9 GSK3β phosphorylation, which inversely correlates with its activity, as well as slightly reduces Cdk5 expression in Tau transgenic mice. Notably, these two kinases target Tau epitopes that were modified by $A_{2A}R$ deletion in THY-Tau22 mice.[29]

We cannot rule out that glial-based phenomena underlie some of the beneficial effects resulting from $A_{2A}R$ blockade. It is known that activation of microglia and pro-inflammatory cytokines promotes Tau hyperphosphorylation[32,44] through kinase activation.[45] $A_{2A}Rs$ are expressed by astroglial and microglial cells, modulating both their activation as well as their ability to release pro-inflammatory factors or to reuptake glutamate.[6,35,46] According to this, A_{2A} receptor blockade has been shown to reduce neuro-inflammation in different pathological situations.[34,47,48] While further studies would be needed to identify the precise underlying mechanisms, our data suggest that $A_{2A}R$ deletion contributes to the reported changes of Tau hyperphosphorylation presumably through a reduction of hippocampal neuroinflammation in THY-Tau22 transgenic mice. Additionally, astrocytes play a key role in regulating adenosine homeostasis and hippocampal plasticity.[49,50] Adenosine metabolic clearance is highly regulated by adenosine kinase, a phosphotransferase predominantly expressed by the astrocytes of the adult brain.[51] Interestingly, astrocytic adenosine kinase upsurge following astrogliosis has been associated with cognitive impairments including hippocampal-dependent memory.[52,53] The fact that $A_{2A}Rs$ play a role in astrocyte activation[6] and that Tau $A_{2A}^{-/-}$ mice exhibit reduced astrogliosis further supports the hypothesis of an astrocyte contribution to the $A_{2A}R$-mediated THY-Tau22 deficits.

In addition to pathological markers, we evaluated the impact of $A_{2A}R$ deletion on neurochemical and synaptic hippocampal indexes. $A_{2A}Rs$ have been shown to modulate neurotransmitter dynamics by regulating both synaptic release and glial uptake.[6,35,36] Regardless of $A_{2A}R$ genotype, we found that THY-Tau22 mice exhibited a limited but significant increase in hippocampal glutamate levels. These observations are in accordance with the somewhat increased vulnerability of these Tau mice when challenged with pentylenetetrazol—a $GABA_A$ receptor antagonist—as well as the abnormal synaptic response of THY-Tau22 slices to bicucullin, another $GABA_A$ receptor antagonist (unpublished data). $A_{2A}Rs$ regulate presynaptic glutamate release as well as glutamate re-uptake by astrocytes.[6,35] Also, A_{2A} receptor blockade in astrocytes is able to counteract β-amyloid toxicity by increasing glutamate uptake.[54] However, we could not observe any changes in glutamate levels following A_{2A} receptor deletion. Rather, we observed that $A_{2A}R$ deletion led to a significant

increase in hippocampal GABA levels in Tau mice. While the differential impact of A_{2A}R deletion on GABA levels in WT and Tau mice remains puzzling, these observations are in line with data reporting regulation of neuronal and glial GABA uptake by A_{2A} Rs.[36,55] Accordingly, we observed a significant decrease of GAT-2 and GAT-3 expression levels in the hippocampus of Tau $A_{2A}^{-/-}$ vs Tau $A_{2A}^{+/+}$ animals. Overall, changes in GABA levels resulted in a normalization of the glutamate/GABA ratio. Previous studies suggested that normalization of the latter could be associated to neuroprotection as well as to memory improvements in various neuropathological models.[56–58]

Finally, behavioural improvements observed in Tau $A_{2A}^{-/-}$ animals were found to be associated with a rescue of hippocampal long-term depression (LTD). As we previously reported in older mice, behavioural deficits seen in THY-Tau22 mice are associated with an impaired LTD,[26] in the absence of neuronal death and synaptic shrinkage.[17] The combined observation of LTD normalization and memory improvement in Tau $A_{2A}^{-/-}$ mice argues for an instrumental role of LTD defect towards cognitive dysfunction in this mouse model. This is in accordance with previous reports linking hippocampal LTD to memory abilities.[59,60] Interestingly, similarly to what has been observed using a specific antagonist,[61] A_{2A}R knockout itself did not impact LTD, in our experimental conditions, in line with the preserved spatial memory of WT $A_{2A}^{-/-}$ animals. The mechanisms underlying LTD normalization in Tau $A_{2A}^{-/-}$ mice remain to be determined. Despite moderate changes, reduced Tau hyperphosphorylation and neuro-inflammation might contribute to the rescue of LTD deficit.[62] Another explanation may rely on GSK3β activity changes. A recent systematic evaluation of the role of kinases in hippocampal LTD revealed that among 58 kinases investigated only GSK3β inhibition was associated with LTD impairments.[63] At first sight, these data are at odds with our observations. However, we demonstrated that, conversely to WT animals, GSK3β inhibition leads to LTD normalization in slices from THY-Tau22 mice (Ahmed *et al.*[64]). Reduced GSK3β activation, besides impacting Tau phosphorylation, could then play a direct role towards the synaptic improvement seen in Tau $A_{2A}^{-/-}$ animals. Finally, the ability of BDNF to impair LTD has recently been demonstrated.[61] The BDNF upsurge described in the hippocampus of THY-Tau22 mice[14] could thus play a role in the LTD impairments seen in this strain. Interestingly, BDNF's effects on LTD were found to be dependent on A_{2A}R activation.[61] It remains thus possible that A_{2A}R deletion in THY-Tau22 mice could gate these BDNF-dependent effects, resulting in LTD normalization. This will deserve further studies.

In conclusion, we have shown for the first time that both A_{2A}R gene deletion and pharmacological blockade are effective in a model of AD-like Tau pathology. Therefore, the present findings highlight A_{2A}R targeting as a promising therapeutic strategy in AD and Tauopathies.

CONFLICT OF INTEREST

The authors declare no conflict of interest.

ACKNOWLEDGMENTS

This work was supported by grants from France Alzheimer (to DB) and LECMA/Alzheimer Forschung Initiative (to DB and CEM). DB and LVL got a Égide/Pessoa program EU exchange grant. Our laboratory is also supported by the LabEx (excellence laboratory) DISTALZ (Development of Innovative Strategies for a Transdisciplinary approach to ALZheimer's disease), Inserm, CNRS, Université Lille 2, Lille Métropole Communauté Urbaine, Région Nord/Pas-de-Calais, FEDER, DN2M, ANR (ADONTAGE and ADORATAU, to DB) and FUI MEDIALZ. We thank the animal facility of IMPRT-IFR114 and M Besegher, I Brion, D Cappe, R Dehaynin, J Devassine, Y Lepage, C Meunier and D Taillieu for transgenic mouse production and animal care, as well as M Basquin, D Demeyer, S Eddarkaoui, H Obriot and M Schneider for support. CL holds a doctoral grant from Lille 2 University, and SB from Région Nord Pas de Calais and CHRU de Lille. VF holds a grant from Région Nord-Pas-de-Calais and Inserm. EF holds a post-doctoral grant from Région Nord-Pas-de-Calais (DN2M). LVL is an Investigator FCT (Fundação para a Ciência e Tecnologia, Portugal).

REFERENCES

1 Flaten V, Laurent C, Coelho J, Sandau U, Batalha VL, Burnouf S *et al.* From epidemiology to pathophysiology: what about caffeine in Alzheimer's disease? *Biochem Soc Trans* 2014; **42**: 587–592.
2 Arendash GW, Schleif W, Rezai-Zadeh K, Jackson EK, Zacharia LC, Cracchiolo JR *et al.* Caffeine protects Alzheimer's mice against cognitive impairment and reduces brain beta-amyloid production. *Neuroscience* 2006; **142**: 941–952.
3 Laurent C, Eddarkaoui S, Derisbourg M, Leboucher A, Demeyer D, Carrier S *et al.* Beneficial effects of caffeine in a transgenic model of Alzheimer's disease-like tau pathology. *Neurobiol Aging* 2014; **35**: 2079–2090.
4 Muller CE, Jacobson KA. Xanthines as adenosine receptor antagonists. *Handbook of Experimental Pharmacology*, 2011, pp 151–199.
5 Blum D, Hourez R, Galas MC, Popoli P, Schiffmann SN. Adenosine receptors and Huntington's disease: implications for pathogenesis and therapeutics. *Lancet Neurol* 2003; **2**: 366–374.
6 Popoli P, Blum D, Martire A, Ledent C, Ceruti S, Abbracchio MP. Functions, dysfunctions and possible therapeutic relevance of adenosine A2A receptors in Huntington's disease. *Progr Neurobiol* 2007; **81**: 331–348.
7 Sebastiao AM, Ribeiro FF, Ribeiro JA. From A1 to A3 en passant through A(2A) receptors in the hippocampus: pharmacological implications. *CNS Neurol Disorders Drug Targets* 2012; **11**: 652–663.
8 Wei CJ, Li W, Chen JF. Normal and abnormal functions of adenosine receptors in the central nervous system revealed by genetic knockout studies. *Biochim Biophys Acta* 2011; **1808**: 1358–1379.
9 Chen JF, Xu K, Petzer JP, Staal R, Xu YH, Beilstein M *et al.* Neuroprotection by caffeine and A(2A) adenosine receptor inactivation in a model of Parkinson's disease. *J Neurosci* 2001; **21**: RC143.
10 Kachroo A, Schwarzschild MA. Adenosine A2A receptor gene disruption protects in an alpha-synuclein model of Parkinson's disease. *Ann Neurol* 2012; **71**: 278–282.
11 Canas PM, Porciuncula LO, Cunha GM, Silva CG, Machado NJ, Oliveira JM *et al.* Adenosine A2A receptor blockade prevents synaptotoxicity and memory dysfunction caused by beta-amyloid peptides via p38 mitogen-activated protein kinase pathway. *J Neurosci* 2009; **29**: 14741–14751.
12 Duyckaerts C, Bennecib M, Grignon Y, Uchihara T, He Y, Piette F *et al.* Modeling the relation between neurofibrillary tangles and intellectual status. *Neurobiol Aging* 1997; **18**: 267–273.
13 Grober E, Dickson D, Sliwinski MJ, Buschke H, Katz M, Crystal H *et al.* Memory and mental status correlates of modified Braak staging. *Neurobiol Aging* 1999; **20**: 573–579.
14 Burnouf S, Belarbi K, Troquier L, Derisbourg M, Demeyer D, Leboucher A *et al.* Hippocampal BDNF expression in a tau transgenic mouse model. *Curr Alzheimer Res* 2012; **9**: 406–410.
15 Van der Jeugd A, Vermaercke B, Derisbourg M, Lo AC, Hamdane M, Blum D *et al.* Progressive age-related cognitive decline in tau mice. *J Alzheimer's Dis* 2013; **37**: 777–788.
16 Ledent C, Vaugeois JM, Schiffmann SN, Pedrazzini T, El Yacoubi M, Vanderhaeghen JJ *et al.* Aggressiveness, hypoalgesia and high blood pressure in mice lacking the adenosine A2a receptor. *Nature* 1997; **388**: 674–678.
17 Burnouf S, Martire A, Derisbourg M, Laurent C, Belarbi K, Leboucher A *et al.* NMDA receptor dysfunction contributes to impaired brain-derived neurotrophic factor-induced facilitation of hippocampal synaptic transmission in a Tau transgenic model. *Aging Cell* 2013; **12**: 11–23.
18 Troquier L, Caillierez R, Burnouf S, Fernandez-Gomez FJ, Grosjean ME, Zommer N *et al.* Targeting phospho-Ser422 by active Tau immunotherapy in the THY-Tau22 mouse model: a suitable therapeutic approach. *Current Alzheimer Research* 2012; **9**: 397–405.
19 Hockemeyer J, Burbiel JC, Müller CE. Multigram-scale syntheses, stability, and photoreactions of A2A adenosine receptor antagonists with 8-styrylxanthine structure: potential drugs for Parkinson's disease. *J Org Chem* 2004; **69**: 3308–3318.
20 Collins LE, Galtieri DJ, Brennum LT, Sager TN, Hockemeyer J, Müller CE *et al.* Oral tremor induced by the muscarinic agonist pilocarpine is suppressed by the adenosine A2A antagonists MSX-3 and SCH58261, but not the adenosine A1 antagonist DPCPX. *Pharmacol Biochem Behav* 2010; **94**: 561–569.
21 Belarbi K, Burnouf S, Fernandez-Gomez FJ, Laurent C, Lestavel S, Figeac M *et al.* Beneficial effects of exercise in a transgenic mouse model of Alzheimer's disease like Tau pathology. *Neurobiol Dis* 2011; **43**: 486–494.
22 Planel E, Richter KE, Nolan CE, Finley JE, Liu L, Wen Y *et al.* Anesthesia leads to tau hyperphosphorylation through inhibition of phosphatase activity by hypothermia. *J Neurosci* 2007; **27**: 3090–3097.

23 Fernandez-Gomez FJ, Jumeau F, Derisbourg M, Burnouf S, Tran H, Eddarkaoui S *et al.* Consensus brain-derived protein, extraction protocol for the study of human and murine brain proteome using both 2D-DIGE and mini 2DE immunoblotting. *J Vis Exp* advance online publication, 10 April 2014; doi:10.3791/51339.
24 Leboucher A, Laurent C, Fernandez-Gomez FJ, Burnouf S, Troquier L, Eddarkaoui S *et al.* Detrimental effects of diet-induced obesity on tau pathology are independent of insulin resistance in tau transgenic mice. *Diabetes* 2013; **62**: 1681–1688.
25 Batalha VL, Pego JM, Fontinha BM, Costenla AR, Valadas JS, Baqi Y *et al.* Adenosine A(2A) receptor blockade reverts hippocampal stress-induced deficits and restores corticosterone circadian oscillation. *Mol Psychiatry* 2013; **18**: 320–331.
26 Van der Jeugd A, Ahmed T, Burnouf S, Belarbi K, Hamdame M, Grosjean ME *et al.* Hippocampal tauopathy in tau transgenic mice coincides with impaired hippocampus-dependent learning and memory, and attenuated late-phase long-term depression of synaptic transmission. *Neurobiol Learn Memory* 2011; **95**: 296–304.
27 Bert L, Favale D, Jego G, Greve P, Guilloux JP, Guiard BP *et al.* Rapid and precise method to locate microdialysis probe implantation in the rodent brain. *J Neurosci Methods* 2004; **140**: 53–57.
28 Sauvinet V, Parrot S, Benturquia N, Bravo-Moraton E, Renaud B, Denoroy L. In vivo simultaneous monitoring of gamma-aminobutyric acid, glutamate, and L-aspartate using brain microdialysis and capillary electrophoresis with laser-induced fluorescence detection: analytical developments and in vitro/in vivo validations. *Electrophoresis* 2003; **24**: 3187–3196.
29 Sergeant N, Bretteville A, Hamdane M, Caillet-Boudin ML, Grognet P, Bombois S *et al.* Biochemistry of Tau in Alzheimer's disease and related neurological disorders. *Expert Rev Proteomics* 2008; **5**: 207–224.
30 Zilka N, Kovacech B, Barath P, Kontsekova E, Novak M. The self-perpetuating tau truncation circle. *Biochem Soc Trans* 2012; **40**: 681–686.
31 Bellucci A, Westwood AJ, Ingram E, Casamenti F, Goedert M, Spillantini MG. Induction of inflammatory mediators and microglial activation in mice transgenic for mutant human P301S tau protein. *Am J Pathol* 2004; **165**: 1643–1652.
32 Lee DC, Rizer J, Selenica ML, Reid P, Kraft C, Johnson A *et al.* LPS- induced inflammation exacerbates phospho-tau pathology in rTg4510 mice. *J Neuroinflamm* 2010; **7**: 56.
33 Bardou I, Brothers HM, Kaercher RM, Hopp SC, Wenk GL. Differential effects of duration and age on the consequences of neuroinflammation in the hippocampus. *Neurobiol Aging* 2013; **34**: 2293–2301.
34 Rebola N, Simoes AP, Canas PM, Tome AR, Andrade GM, Barry CE *et al.* Adenosine A2A receptors control neuroinflammation and consequent hippocampal neuronal dysfunction. *J Neurochem* 2011; **117**: 100–111.
35 Matos M, Augusto E, Agostinho P, Cunha RA, Chen JF. Antagonistic interaction between adenosine A2A receptors and Na+/K+-ATPase-alpha2 controlling glutamate uptake in astrocytes. *J Neurosci* 2013; **33**: 18492–18502.
36 Cristovao-Ferreira S, Navarro G, Brugarolas M, Perez-Capote K, Vaz SH, Fattorini G *et al.* A1R-A2AR heteromers coupled to Gs and G i/0 proteins modulate GABA transport into astrocytes. *Purinergic Signal* 2013; **9**: 433–449.
37 Albasanz JL, Perez S, Barrachina M, Ferrer I, Martin M. Up-regulation of adenosine receptors in the frontal cortex in Alzheimer's disease. *Brain Pathol* 2008; **18**: 211–219.
38 Zhou SJ, Zhu ME, Shu D, Du XP, Song XH, Wang XT *et al.* Preferential enhancement of working memory in mice lacking adenosine A(2A) receptors. *Brain Res* 2009; **1303**: 74–83.
39 Wei CJ, Singer P, Coelho J, Boison D, Feldon J, Yee BK *et al.* Selective inactivation of adenosine A(2A) receptors in striatal neurons enhances working memory and reversal learning. *Learn Memory* 2011; **18**: 459–474.
40 Leite MR, Wilhelm EA, Jesse CR, Brandao R, Nogueira CW. Protective effect of caffeine and a selective A2A receptor antagonist on impairment of memory and oxidative stress of aged rats. *Exp Gerontol* 2011; **46**: 309–315.
41 Ning YL, Yang N, Chen X, Xiong RP, Zhang XZ, Li P *et al.* Adenosine A2A receptor deficiency alleviates blast-induced cognitive dysfunction. *J Cerebr Blood Flow Metab* 2013; **33**: 1789–1798.
42 Le Freche H, Brouillette J, Fernandez-Gomez FJ, Patin P, Caillierez R, Zommer N *et al.* Tau phosphorylation and sevoflurane anesthesia: an association to postoperative cognitive impairment. *Anesthesiology* 2012; **116**: 779–787.
43 Santacruz K, Lewis J, Spires T, Paulson J, Kotilinek L, Ingelsson M *et al.* Tau suppression in a neurodegenerative mouse model improves memory function. *Science* 2005; **309**: 476–481.
44 Gorlovoy P, Larionov S, Pham TT, Neumann H. Accumulation of tau induced in neurites by microglial proinflammatory mediators. *FASEB J* 2009; **23**: 2502–2513.
45 Kitazawa M, Oddo S, Yamasaki TR, Green KN, LaFerla FM. Lipopolysaccharide-induced inflammation exacerbates tau pathology by a cyclin-dependent kinase 5-mediated pathway in a transgenic model of Alzheimer's disease. *J Neurosci* 2005; **25**: 8843–8853.
46 Orr AG, Orr AL, Li XJ, Gross RE, Traynelis SF. Adenosine A(2A) receptor mediates microglial process retraction. *Nature Neurosci* 2009; **12**: 872–878.
47 Dai SS, Zhou YG, Li W, An JH, Li P, Yang N *et al.* Local glutamate level dictates adenosine A2A receptor regulation of neuroinflammation and traumatic brain injury. *J Neurosci* 2010; **30**: 5802–5810.
48 Yu L, Shen HY, Coelho JE, Araujo IM, Huang QY, Day YJ *et al.* Adenosine A2A receptor antagonists exert motor and neuroprotective effects by distinct cellular mechanisms. *Ann Neurol* 2008; **63**: 338–346.
49 Pascual O, Casper KB, Kubera C, Zhang J, Revilla-Sanchez R, Sul JY *et al.* Astrocytic purinergic signaling coordinates synaptic networks. *Science* 2005; **310**: 113–116.
50 Boison D. Adenosine dysfunction in epilepsy. *Glia* 2012; **60**: 1234–1243.
51 Studer FE, Fedele DE, Marowsky A, Schwerdel C, Wernli K, Vogt K *et al.* Shift of adenosine kinase expression from neurons to astrocytes during postnatal development suggests dual functionality of the enzyme. *Neuroscience* 2006; **142**: 125–137.
52 Shen HY, Singer P, Lytle N, Wei CJ, Lan JQ, Williams-Karnesky RL *et al.* Adenosine augmentation ameliorates psychotic and cognitive endophenotypes of schizophrenia. *J Clin Invest* 2012; **122**: 2567–2577.
53 Yee BK, Singer P, Chen JF, Feldon J, Boison D. Transgenic overexpression of adenosine kinase in brain leads to multiple learning impairments and altered sensitivity to psychomimetic drugs. *Eur J Neurosci* 2007; **26**: 3237–3252.
54 Matos M, Augusto E, Machado NJ, dos Santos-Rodrigues A, Cunha RA, Agostinho P. Astrocytic adenosine A2A receptors control the amyloid-β peptide-induced decrease of glutamate uptake. *J Alzheimers Dis* 2012; **31**: 555–567.
55 Cristovao-Ferreira S, Vaz SH, Ribeiro JA, Sebastiao AM. Adenosine A2A receptors enhance GABA transport into nerve terminals by restraining PKC inhibition of GAT-1. *J Neurochem* 2009; **109**: 336–347.
56 Xu XH, Zheng XX, Zhou Q, Li H. Inhibition of excitatory amino acid efflux contributes to protective effects of puerarin against cerebral ischemia in rats. *Biomed Environ Sci* 2007; **20**: 336–342.
57 Dong X, Zhang D, Zhang L, Li W, Meng X. Osthole improves synaptic plasticity in the hippocampus and cognitive function of Alzheimer's disease rats via regulating glutamate. *Neural Regen Res* 2012; **7**: 2325–2332.
58 Luo J, Min S, Wei K, Li P, Dong J, Liu YF. Propofol protects against impairment of learning-memory and imbalance of hippocampal Glu/GABA induced by electroconvulsive shock in depressed rats. *J Anesth* 2011; **25**: 657–665.
59 Altinbilek B, Manahan-Vaughan D. Antagonism of group III metabotropic glutamate receptors results in impairment of LTD but not LTP in the hippocampal CA1 region, and prevents long-term spatial memory. *Eur J Neurosci* 2007; **26**: 1166–1172.
60 Dong Z, Bai Y, Wu X, Li H, Gong B, Howland JG *et al.* Hippocampal long-term depression mediates spatial reversal learning in the Morris water maze. *Neuropharmacology* 2013; **64**: 65–73.
61 Rodrigues TM, Jeronimo-Santos A, Sebastiao AM, Diogenes MJ. Adenosine A(2A) receptors as novel upstream regulators of BDNF-mediated attenuation of hippocampal long-term depression (LTD). *Neuropharmacology* 2014; **79**: 389–398.
62 Min SS, Quan HY, Ma J, Han JS, Jeon BH, Seol GH. Chronic brain inflammation impairs two forms of long-term potentiation in the rat hippocampal CA1 area. *Neurosci Lett* 2009; **456**: 20–24.
63 Peineau S, Nicolas CS, Bortolotto ZA, Bhat RV, Ryves WJ, Harwood AJ *et al.* A systematic investigation of the protein kinases involved in NMDA receptor-dependent LTD: evidence for a role of GSK-3 but not other serine/threonine kinases. *Mol Brain* 2009; **2**: 22.
64 Ahmed T, Blum D, Burnouf S, Demeyer D, Buée-Scherrer V, D'Hooge R *et al.* Inhibition of GSK3β and activation of PP2A rescue defects in NMDAR-mediated late phase LTD in a Tau transgenic mouse model. *Neurobiology of Aging* (in press).

Supplementary Information accompanies the paper on the Molecular Psychiatry website (http://www.nature.com/mp)